*J. Fluid Mech.* (1986), *vol.* 172, *pp.* 547–563
*Printed in Great Britain*



# Highest waves, phase speeds and particle trajectories of nonlinear capillary waves on sheets of fluid

By S. J. HOGAN
Mathematical Institute, University of Oxford, 24/29 St Giles, Oxford OX1 3LB

(Received 18 February 1985 and in revised form 12 May 1986)

We derive exact criteria for the highest capillary waves on sheets of fluid and present the profiles for both symmetric and antisymmetric waves. In addition we provide correct definitions of the phase speed of these waves. Previous 'essentially nonlinear' solutions to the problem are shown to have been misinterpreted.

Trajectory properties of particles in both types of wave are presented. We also give results for the drift velocity ratios as a function of the mean displacement of a streamline from the free surface. Many of the results are exact, being given in terms of elliptic functions and elliptic integrals. An application to wave motion in thin films on pipe walls is considered.

## 1. Introduction

Two recent papers by the present author have considered the particle trajectories in nonlinear waves influenced by surface tension and gravity. In the first (Hogan 1984) gravity was neglected entirely and an exact solution for the wave profile due to Crapper (1957) was used in the calculations. In the second paper (Hogan 1985*a*), both restoring forces were included and computer generated solutions were used. Both these papers considered the wave motion on an ideal fluid of infinite depth.

The present paper is a further generalization of Hogan (1984). Gravity is neglected but the effect of the depth of the fluid is considered. Kinnersley (1976) has conducted an investigation into the shape of the wave profile in this case, with nonlinearity fully taken into account. He found not one generalization of Crapper's (1957) solution but two, corresponding to symmetric and antisymmetric waves on a fluid sheet. He derived exact expressions for the profiles, in terms of elliptic functions and elliptic integrals. Taylor (1959) had originally calculated the linear form of these waves. We use Kinnersley's results here in the same manner as Crapper's (1957) results were used by Hogan (1984).

In §2 we introduce the work of Kinnersley (1976) and describe the problem. In §3 we extend his work to give exact criteria for highest waves and present them in graphical form for the first time. It is shown in §4 that Kinnersley's parameter $c$ is not equivalent to either definition of the phase speed as given by Stokes (1847). This leads to the intriguing result that symmetric waves on a very thin sheet of fluid have zero phase speed. We present trajectory results as seen in two different reference frames in §5 and examine their connection with results from Hogan (1984). In §6 the trajectories and drift velocity ratios are presented in graphical form. We discuss these results in §7.

## 2. The work of Kinnersley (1976)

It was Taylor (1959) who first showed that there are two types of capillary wave possible on the surface of a fluid sheet. One type is symmetric and the other type antisymmetric with respect to the centreline of the sheet. Taylor's analysis was valid only for small amplitude. In the limit of a very thin sheet, he showed that the antisymmetric waves were non-dispersive. He confirmed his theoretical observations in a series of elegant experiments.

Kinnersley (1976) relaxed the assumption of small amplitude and was able to derive exact solutions involving elliptic functions and elliptic integrals. In the limit of sheet thickness tending to infinity, both solutions tend to the nonlinear solution of Crapper (1957), whose method of solution Kinnersley used.

Kinnersley considered steady, symmetric, periodic nonlinear capillary waves which propagate on the surface of a sheet of incompressible inviscid fluid of finite thickness. The motion in the fluid is two-dimensional and irrotational and the wave is moving to the right. By moving in a suitable frame of reference, the flow is reduced to a steady state whose Cartesian axes are chosen with $x$ measured horizontally to the left (upstream) and $y$ vertically downwards. We use Kinnersley's notation throughout, including the convention that the modulus of elliptic functions is omitted, since all functions of velocity potential $\phi$ have modulus $k$ and all functions of stream function $\psi$ have modulus $k'$, where $k^2+k'^2=1$. The centreline of the sheet is given by $\psi=0$ and the free surface by $\psi=\pm B$. Over one crest-to-crest wavelength $\phi$ ranges from 0 to $4K(k)$ where $K(k)$ is the complete elliptic integral of the first kind.

For symmetric waves (case I$b$), Kinnersley found that relative to axes moving with speed $c$,

$$x=\frac{S}{\rho c^2 A k'^2}\left[2E(\phi)-k'^2\phi-2k^2\,\mathrm{sn}\,\phi\,\mathrm{cd}\,\phi+\frac{2kk'^2\,\mathrm{sd}\,\phi\,\mathrm{nd}\,\phi}{\mathrm{dn}\,\psi-k\,\mathrm{cd}\,\phi}\right], \tag{2.1}$$

$$y=\frac{S}{\rho c^2 A k'^2}\left[(1+k^2)\,\psi-2E(\psi)+\frac{2k'^2\,\mathrm{sn}\,\psi\,\mathrm{cn}\,\psi}{\mathrm{dn}\,\psi-k\,\mathrm{cd}\,\phi}\right], \tag{2.2}$$

where we denote the surface tension by $S$ and the density by $\rho$. $E(\phi)$ is the incomplete elliptic function of the second kind. The parameter $A$ is related to the free surface $\psi=\pm B$ by Kinnersley's equation (36). The wavelength $\lambda$, crest-to-trough amplitude $a$ and depth, or sheet semi-thickness, $h$ (defined as the distance from centreline to free surface trough) are given by his equations (35), (38) and (39). The parameter $c$ is given by his equation (40), although we shall see later that $c$ does not equal either accepted definition of the phase speed.

For antisymmetric waves (case II$b$), he found

$$x=\frac{S}{\rho c^2 A}\left[2E(\phi)-\phi+\frac{2k\,\mathrm{sn}\,\phi\,\mathrm{dn}\,\phi}{\mathrm{ds}\,\psi-k\,\mathrm{cn}\,\phi}\right], \tag{2.3}$$

$$y=\frac{S}{\rho c^2 A}\left[-2E(\psi)+\psi-2\,\mathrm{dn}\,\psi\,\mathrm{cs}\,\psi+\frac{2\,\mathrm{ns}\,\psi\,\mathrm{cs}\,\psi}{\mathrm{ds}\,\psi-k\,\mathrm{cn}\,\phi}\right], \tag{2.4}$$

where $\lambda, a, h$ and $c$ are given in this case by Kinnersley's equations (43), (46), (47) and (49). The parameter $A$ is related to $B$ by his equation (44).†

† $k\to 0$ corresponds to finite amplitude waves on water of great depths unless $\psi$ is small and $\psi\to 0$ corresponds to waves on a thin sheet unless $k$ is small. Taylor's (1959) results correspond to having both $k$ and $\psi$ small.

Crapper's (1957) solution (case III of Kinnersley) is given in this notation by

$$x = \frac{S}{\rho c^2 A}\left[\phi + \frac{2\sin\phi}{\cosh\psi - \cos\phi}\right], \tag{2.5}$$

$$y = \frac{S}{\rho c^2 A}\left[\psi - \frac{2\sinh\psi}{\cosh\psi - \cos\phi}\right]. \tag{2.6}$$

The parameter $A$ is not identical to Crapper's $A$, but they are simply related.†

The purpose of this paper is to investigate the particle trajectories of waves described by (2.1)–(2.4), in a similar manner to the investigation by Hogan (1984) of waves described by (2.5)–(2.6). We also give criteria for the highest waves.

Finally we note that Kinnersley derived his solutions under the assumption that each streamline within the fluid could be a free surface if the fluid above is removed. Thus it is sufficient to consider only the highest wave and its streamlines in each case.

## 3. Highest waves

In each of the above cases, the waveform has a maximum amplitude which occurs when the free surface touches itself to enclose a bubble, usually in the trough. We can put this criterion in explicit form by noting that we require a vertical tangent at $x = \frac{1}{2}\lambda$ for $\phi \neq 2K$.

For case I$b$, we require

$$L^2 - 2(1+k^2) = 2L\,\mathrm{cn}\,\phi\,\mathrm{ds}\,\phi, \tag{3.1}$$

where

$$L(\phi) = 4E - 2E(\phi) + k'^2\phi - 2k'^2K. \tag{3.2}$$

Here $E = E(k)$ is the complete elliptic integral of the second kind. We solve (3.1)–(3.2) by fixing $k$ and finding a solution for $\phi(\neq 2K$, which corresponds to the trough). The value of $B = B_{\max}$ corresponding to the highest wave is then found from

$$\mathrm{dn}\,B_{\max} = \frac{k(L\,\mathrm{cd}\,\phi + 2\,\mathrm{sn}\,\phi)}{L + 2k^2\,\mathrm{sn}\,\phi\,\mathrm{cd}\,\phi}. \tag{3.3}$$

For case II$b$, we fix $k$ and solve for $\phi(\neq 2K)$ from

$$I^2\,\mathrm{sn}\,\phi\,\mathrm{dn}\,\phi = 2(2\,\mathrm{dn}^2\phi - 1)[I\,\mathrm{cn}\,\phi + \mathrm{sn}\,\phi\,\mathrm{dn}\,\phi], \tag{3.4}$$

where

$$I(\phi) = 4E - 2E(\phi) + \phi - 2K, \tag{3.5}$$

and we find the maximum value of $B$ from

$$\mathrm{ds}\,B_{\max} = \frac{k(I\,\mathrm{cn}\,\phi + 2\,\mathrm{sn}\,\phi\,\mathrm{dn}\,\phi)}{I}. \tag{3.6}$$

Equations (3.3) and (3.6) are obtained simply by setting $x = \frac{1}{2}\lambda$.

When $k \to 0$, both these criteria tend to Crapper's (1957) equation (67), with a suitable adjustment to the origin of $\phi$.

We present highest-wave profiles in figures 1 and 2. Figure 1 ($a$) contains profiles for the symmetric wave (case I$b$) with $k = 0.25$ and figure 1 ($b$) with $k = 0.75$. For this case, the highest wave in the limit $k = 1$ corresponds to $a/\lambda = 0.5$, $a/h$ infinite and $\tan B_{\max} = 1$ ($B_{\max} = \frac{1}{4}\pi$). It is represented by a semicircle. In figure 1, the full wave is obtained by direct reflection in the line $B = 0$. For the antisymmetric waves

† Equation (2.4) of Hogan (1984) and equation (2.2) of Hogan (1985$b$) both contain an incorrect factor ($S/\rho k$). The correct factor should be ($Sk/\rho$).

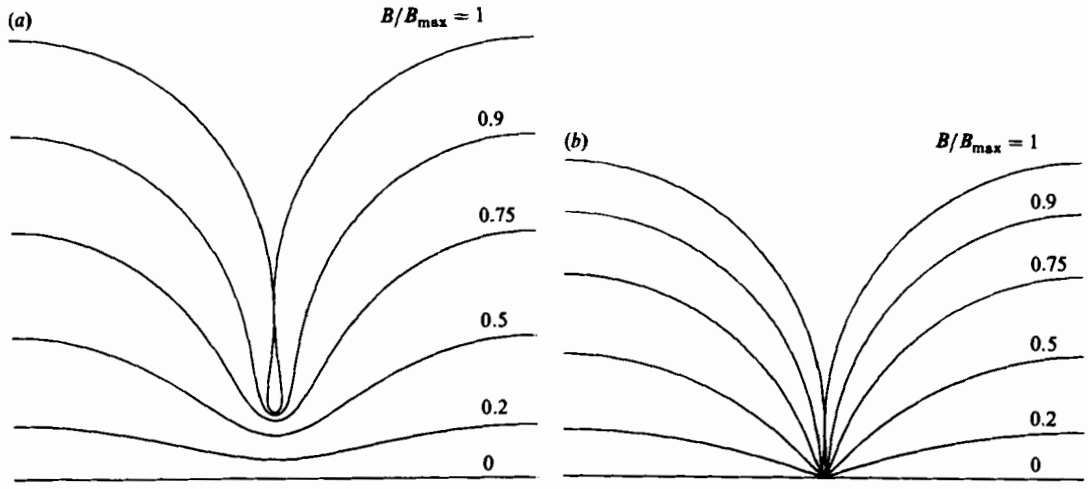


FIGURE 1. (*a*) Symmetric ($k = 0.25$) capillary wave streamlines for $B/B_{max} = 1$, 0.9, 0.75, 0.5, 0.2 and 0, ($B_{max} = 2.014007$). (*b*) Symmetric ($k = 0.75$) capillary wave streamlines for $B/B_{max} = 1$, 0.9, 0.75, 0.5, 0.2 and 0, ($B_{max} = 1.022780$).

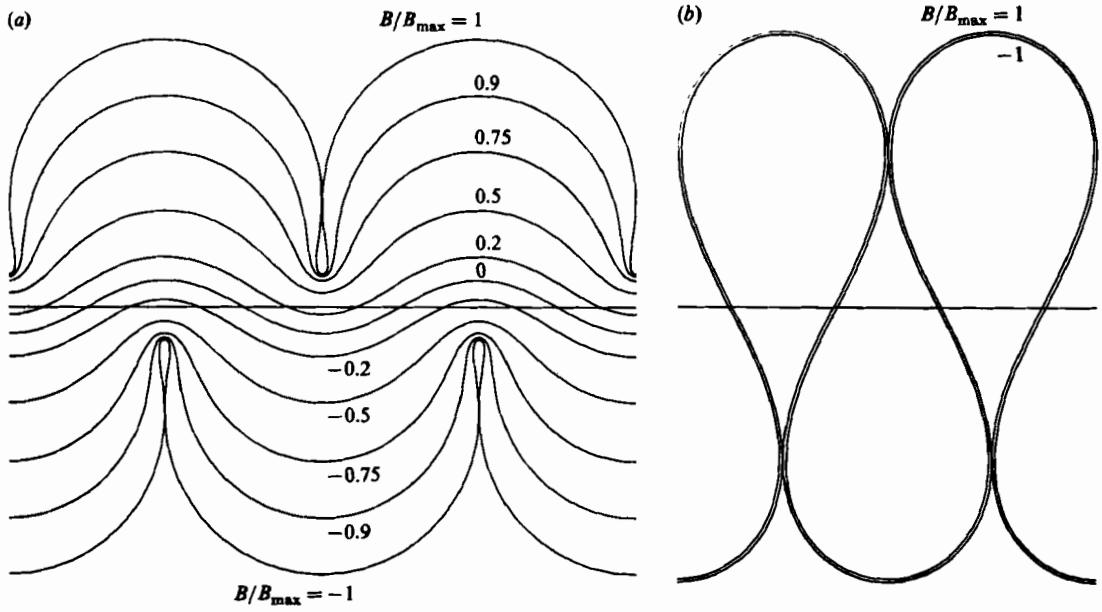


FIGURE 2. (*a*) Antisymmetric ($k = 0.25$) capillary wave streamlines for $B/B_{max} = \pm 1$, $\pm 0.9$, $\pm 0.75$, $\pm 0.5$, $\pm 0.2$ and 0, ($B_{max} = 1.986029$). (*b*) Antisymmetric ($k = 0.854$) capillary wave streamlines for $B/B_{max} = \pm 1$, ($B_{max} = 0.009685$).

(case II*b*) the value $k = 1$ is not reached. Thus in figure 2(*a*) we show the highest-wave profile and streamlines for $k = 0.25$ and in figure 2(*b*) for $k = 0.854$. In both cases we have included the line $y = 0$ for reference only. There is clearly a limit to the value of $k$ corresponding to the trough bubble on top meeting the crest bubble underneath. We find this equivalent to $B_{max} = 0$, $k = 0.858517$, $a/\lambda = 2.820646$. These limiting

values for $k$ and $a/\lambda$ are higher than those given by Kinnersley ($k^2 = 0.73, a/\lambda = 2.7$). Here the highest-wave criterion reduces to $I = 0$, from (3.6), which Kinnersley's values do not satisfy exactly.

## 4. Phase speeds

In this section we show that the parameter $c$ in Kinnersley's work does not equal either definition of the phase speed, as given by Stokes (1847).

Kinnersley derives velocity components $u_K, v_K$ relative to a frame of reference in which the wave profile is steady. Thus the horizontal velocity $u$ relative to the laboratory is given by

$$u + c_p = u_K, \tag{4.1}$$

where $c_p$ is the speed of the wave crests.

Now if we denote an average over one wavelength as an overbar defined by

$$\overline{(\ldots)} = \frac{1}{\lambda}\int_0^\lambda (\ldots)\,\mathrm{d}x, \tag{4.2}$$

then from Stokes (1847) we can immediately write, since the motion is irrotational,

$$c_p = \bar{u}_K|_{B=0}, \tag{4.3}$$

independent of the wave symmetry.

For case I$b$ we find, from Kinnersley,

$$\frac{c_p}{c} = \frac{k'^2 K}{(2E - k'^2 K)}, \tag{4.4}$$

and for case II$b$,

$$\frac{c_p}{c} = \frac{(4k^2-1)\,K + 4(1-2k^2)\,E}{3(2E-K)}. \tag{4.5}$$

Thus in general $c \neq c_p$. We note that when $k = 0$, that is for fluid of great depths, we find $c_p = c$ in both cases, confirming Crapper's (1957) choice of integration constant for Bernoulli's equation. In addition we find for $k \approx 1$ that (4.4) gives us for case I$b$ (symmetric) waves

$$\frac{c_p}{c} \approx \frac{k'^2}{2}\ln\frac{4}{k'}, \tag{4.6}$$

and so $c_p/c = 0$ for $k = 1$. For case II$b$ (antisymmetric) waves the limiting case $k = 0.858517$ corresponds to $c_p/c = 2.020924$.

Stokes (1847) gave another definition for the phase speed of waves which we will denote by $c_q$. It is given by

$$c_q \equiv \frac{\iint u_K\,\mathrm{d}y\,\mathrm{d}x}{\iint \mathrm{d}y\,\mathrm{d}x}. \tag{4.7}$$

Thus $c_q$ is the mean horizontal velocity of the centre of mass of the wave. For a fluid of infinite depth $c_p = c_q$, but in general they are unequal. We can evaluate $c_q$ analytically for all values of $k$. We transform to the $(\phi, \psi)$-plane and this introduces a Jacobian $1/q^2$ into both integrands where $q^2 = u_K^2 + v_K^2$ is the particle speed. The quantities $u_K$ and $q^2$ are given in equations (27) and (28), using table 1, of Kinnersley.

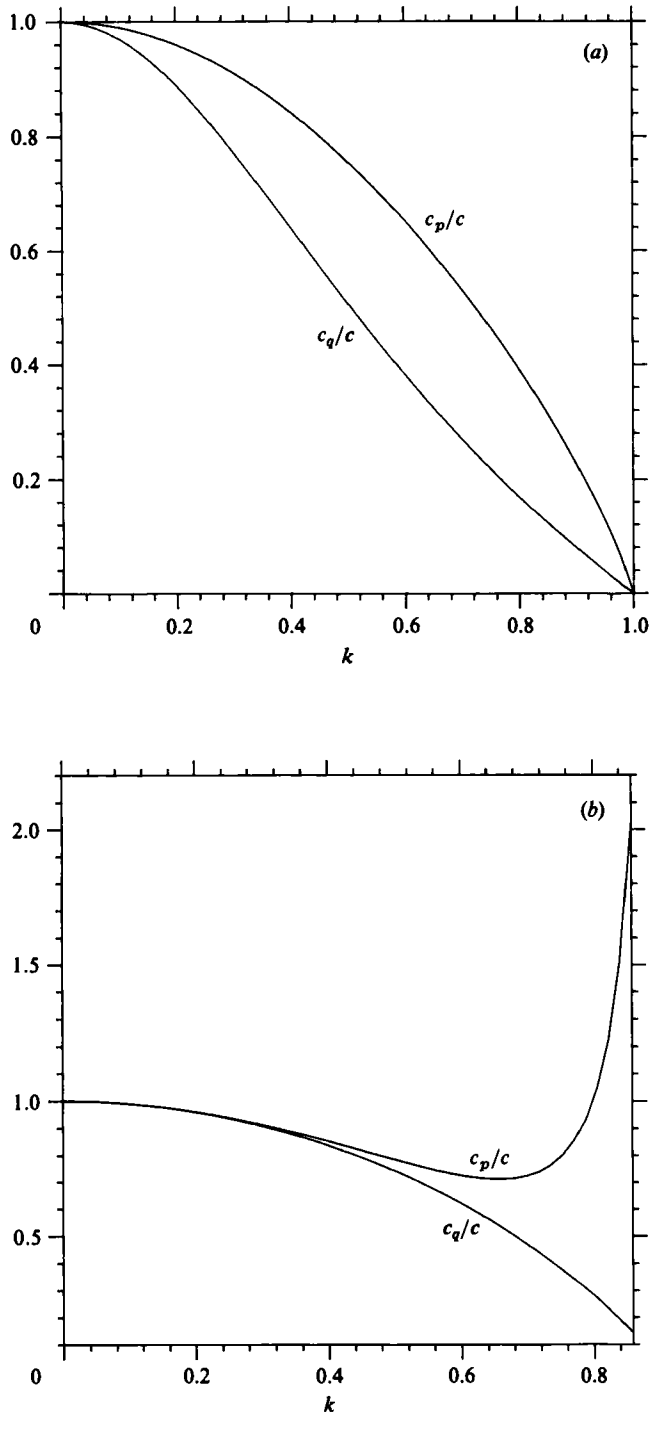


FIGURE 3. (*a*) The ratios $c_p/c$ and $c_q/c$ as a function of $k$ for symmetric waves. (*b*) As figure 3(*a*), for antisymmetric waves.

Since the flow is irrotational it is sufficient to evaluate both integrands at $B = 0$. The resulting integrals are then very simple to perform. Thus for case I$b$ we find

$$\frac{c_q}{c} = \frac{3k'^2(2E - k'^2K)}{[8(1+k^2)E - (5+3k^2)k'^2K]}, \tag{4.8}$$

and for case II$b$

$$\frac{c_q}{c} = \frac{2E-K}{K}. \tag{4.9}$$

In addition for $k \approx 1$, we find from (4.8) that

$$\frac{c_q}{c} \approx \tfrac{3}{8}k'^2. \tag{4.10}$$

Thus $c_q/c = 0$ when $k = 1$ for symmetric waves. For antisymmetric waves, the limiting case $k = 0.858517$ has $c_q/c = 0.142634$. In general $c \neq c_q$.

In figure 3($a$) we have plotted $c_p/c$ and $c_q/c$ *vs.* $k$ for case I$b$ (symmetric waves). Similarly in figure 3($b$) we have plotted $c_p/c$ and $c_q/c$ *vs.* $k$ for case II$b$ (antisymmetric) waves. We note that in this case $c_p \approx c_q$ for $k$ as large as 0.3.

In general $c$ does not equal either definition of the phase speed, as given by Stokes (1847).

## 5. Trajectory properties

We calculate the particle trajectories in two frames of reference. In frame $P$, the phase speed of the waves is $c_p$ and in frame $Q$ it is $c_q$. The cartesian axes of these frames are $(X_p, Y)$ and $(X_q, Y)$ where

$$X_p = x - c_p t, \quad X_q = x - c_q t, \quad Y = y, \tag{5.1}$$

and so we must calculate $t$, the time taken by the particle to move from $\phi = \phi_1$ to $\phi = \phi_2$ along a streamline $\psi = \psi_c$. From Longuet-Higgins (1979 §3) we know that

$$t = \int_{\phi_1}^{\phi_2} \left|\frac{\mathrm{d}z}{\mathrm{d}\chi}\right|^2_{\psi=\psi_c} \mathrm{d}\phi, \tag{5.2}$$

where $z = x + \mathrm{i}y$ and $\chi = \phi + \mathrm{i}\psi$.

Since any streamline of the waves under consideration can be regarded as a free surface we set $\psi_c = B$ and let $B$ vary between 0 and $B_{\max}$.

Thus for case I we must evaluate

$$t_{\mathrm{I}} = \frac{S}{\rho c^3 A} \int \left(\frac{1+\alpha\,\mathrm{cd}\,\phi}{1-\alpha\,\mathrm{cd}\,\phi}\right)^2 d\phi, \tag{5.3}$$

where $\alpha = \mathrm{dn}\,B$ for case I$a$ and $\alpha = k\,\mathrm{nd}\,B$ for case I$b$.

For case II the required integral is

$$t_{\mathrm{II}} = \frac{S}{\rho c^3 A} \int \left(\frac{1+\beta\,\mathrm{cn}\,\phi}{1-\beta\,\mathrm{cn}\,\phi}\right)^2 \mathrm{d}\phi \tag{5.4}$$

and here $\beta = \mathrm{cn}\,B$ for case II$a$ and $\beta = k\,\mathrm{sd}\,B$ for case II$b$. Thus in general we have $t = (S/\rho c^3 A)J$.

It is possible to evaluate both these integrals in terms of known functions with due care being taken with the limits $B = 0$, $k = 0$ and $k = 1$. Extensive use is made of formulae given in Byrd & Friedman (1971).

We find for case I,

$$J=\frac{[k^4(1-\alpha^2)+2k^2\alpha^2(3-\alpha^2)-\alpha^4(3+\alpha^2)]}{(1-\alpha^2)(k^2-\alpha^2)^2}\phi-\frac{4\alpha^2}{(1-\alpha^2)(k^2-\alpha^2)}E(\phi)$$
$$+\frac{4\alpha^2k'^2(\alpha^4-k^2)}{(1-\alpha^2)^2(\alpha^2-k^2)^2}\Pi\left(\phi,\alpha_1^2\right)$$
$$+\frac{4\alpha^2\,\mathrm{sn}\,\phi}{(1-\alpha^2)^2(\alpha^2-k^2)(1-\alpha_1^2\,\mathrm{sn}^2\,\phi)}[(\alpha^2-k^2)\,\mathrm{cn}\,\phi\,\mathrm{dn}\,\phi+\alpha k'^2]$$
$$+\frac{4\alpha(\alpha^4-k^2)}{(1-\alpha^2)(\alpha^2-k^2)}\left(\frac{(1-\alpha^2)}{(\alpha^2-k^2)}\right)^{\frac{1}{2}}\tan^{-1}\left\{\left(\frac{\alpha^2-k^2}{1-\alpha^2}\right)^{\frac{1}{2}}\mathrm{sn}\,\phi\right\}, \tag{5.5}$$

where $\alpha_1^2=(k^2-\alpha^2)/(1-\alpha^2)$ and $\Pi(\phi,\alpha_1^2)$ is the incomplete elliptic integral of the third kind. The limit $B=0$ is well-behaved but the explicit form of $t_{\mathrm{I}}$ is not needed in this case. The limit $k=0$ can be shown to be equivalent to equation (4.15) of Hogan (1984). Equation (5.5) has also been checked by direct differentiation.

For case II, we obtain

$$J=\frac{1}{(1-\beta^2)^2}\left\{(\beta^2-1)(\beta^2+3)\phi+\frac{4\beta^2}{(k^2-\beta_1^2)}E(\phi)\right.$$
$$+4(\beta^2-1)\frac{(2\beta_1^2k^2-\beta_1^4-k^2)}{(k^2-\beta_1^2)}\Pi(\phi,\beta_1^2)+\frac{4\beta^3\,\mathrm{sn}\,\phi\,\mathrm{dn}\,\phi}{(k^2-\beta_1^2)(1-\beta\,\mathrm{cn}\,\phi)}$$
$$\left.+\frac{4\beta[k^2(1+\beta^2)-\beta^2\beta_1^2]}{(k^2-\beta_1^2)}\left(\frac{(1-\beta^2)}{(k^2+k'^2\beta^2)}\right)^{\frac{1}{2}}\tan^{-1}\left\{\left(\frac{(k^2+k'^2\beta^2)}{(1-\beta^2)}\right)^{\frac{1}{2}}\mathrm{sd}\,\phi\right\}\right\}, \tag{5.6}$$

where $\beta_1^2=\beta^2/(\beta^2-1)$.

The limit $B\to0$ is straightforward. The limit $k\to0$ behaves just as for case I and (5.6) has been checked by direct differentiation.

The total time, $T$, taken to complete one orbit is obtained by evaluating $t$ between the points $\phi=0$ and $\phi=4K$. In this way we find the time-averaged drift velocity $U$, given by

$$\frac{U_p}{c_p}=1-\frac{\lambda}{c_pT},\quad \frac{U_q}{c_q}=1-\frac{\lambda}{c_qT}, \tag{5.7}$$

and the distance through which a particle moves in one orbit, $[X]$, given by

$$\frac{[X_p]}{\lambda}=\frac{c_pT}{\lambda}-1,\quad \frac{[X_q]}{\lambda}=\frac{c_qT}{\lambda}-1. \tag{5.8}$$

Following Kinnersley, we restrict our attention now to cases I$b$ and II$b$. Thus we find for example

$$\frac{c_pT_{\mathrm{I}}}{\lambda}=\frac{K\,\mathrm{nc}^4B\,\mathrm{ns}^4B}{k'^2(2E-k'^2K)^2}\{4\,\mathrm{dn}^2B(k^2-\mathrm{dn}^4B)\Pi(\alpha_1^2)+4k'^2\,\mathrm{dn}^2B\,\mathrm{cn}^2B\,\mathrm{sn}^2B\mathrm{E}$$
$$+\mathrm{cn}^2B(k'^2\,\mathrm{cn}^2B\,\mathrm{dn}^4B+2\,\mathrm{dn}^2B(3\,\mathrm{dn}^2B-k^2)-(3\,\mathrm{dn}^2B+k^2))K\}, \tag{5.9}$$

where $\alpha_1^2=-k^2\,\mathrm{sc}^2B$ and

$$\frac{c_pT_{\mathrm{II}}}{\lambda}=\frac{\mathrm{nc}^4B}{3(2E-K)^2}[(4k^2-1)K+4(1-2k^2)E]\{4\,\mathrm{dn}^2B(\mathrm{dn}^4B+k^2k'^2\,\mathrm{sn}^4B)\Pi(\alpha_1^2)$$
$$+4\,\mathrm{dn}^2B\,\mathrm{cn}^2B\,\mathrm{sn}^2BE-\mathrm{cn}^2B(k^2\,\mathrm{sn}^2B+3\,\mathrm{dn}^2B)K\}. \tag{5.10}$$

We note that in both (5.9) and (5.10) all the elliptic integrals are complete.

When $B = 0$, (5.9) becomes

$$\frac{c_p T_{\mathrm{I}}}{\lambda} = \frac{[(3k^2+5)\,k'^2K - 8(k^2+1)\,E]\,K}{3(2E-k'^2K)^2}, \tag{5.11}$$

and (5.10) becomes

$$\frac{c_p T_{\mathrm{II}}}{\lambda} = \frac{[(4k^2-1)\,K + 4(1-2k^2)\,E]\,K}{3(2E-K)^2}. \tag{5.12}$$

Once we have calculated $t$ it is a straightforward matter to calculate the trajectory properties from (2.1)–(2.4), (4.4), (4.5), (4.7), (5.5) and (5.6). In the limit $k \to 0$, $B \to 0$, the expressions for $(X, Y)$ yield ellipses.

Immediately we note from (4.4), (4.5), (4.8), (4.9), (5.11) and (5.12) that $c_q T/\lambda = 1$ for both case I$b$ and II$b$ for all $k$ when $B = 0$. Thus in this special case $[X_q]/\lambda = 0$ and $U_q/c_q = 0$.

We also wish to know the behaviour of the time-averaged drift velocity ratios $U_p/c_p$ and $U_q/c_q$ as a function of the mean displacement of a streamline from the free surface, $(\bar{y}_0 - \bar{y}_c)/\lambda$, where $y_0 = y(\psi = 0)$, $y_c = y(\psi = B)$. It is possible to perform the integration to obtain $\bar{y}$ exactly and express the result in terms of elliptic integrals. But the resulting expression is extremely lengthy and the amount of algebra excessive. Thus this calculation was performed numerically with a standard integration routine (NAGLIB D01AJF). The integral converged well in all cases, even for case I$b$ with $k$ nearly equal to 1.

When $k = 1$ for case I$b$, the streamlines are ellipses

$$\left(\frac{2x}{\lambda}\right)^2 = \left(1 - \frac{y}{a}\right)\left(1 + \frac{y}{a}\tan^2 B\right), \tag{5.13}$$

where $a/\lambda = \frac{1}{2}\tan B$. The limiting wave occurs when $\tan B = 1$.

In this case, we can derive a simple exact expression for the quantity $(\bar{y}_0 - \bar{y}_c)/\lambda$, namely

$$\frac{(\bar{y}_0 - \bar{y}_c)}{\lambda} = -\frac{1}{8}\left\{\pi + \frac{(\sin 4B - 4B)}{\sin^2 2B}\right\}. \tag{5.14}$$

## 6. Results

We shall discuss the trajectory profiles and the time-averaged drift velocity ratios in both reference frames $P$ and $Q$.

For symmetric waves (case I$b$) with $k = 0.25$, trajectory profiles are given in figures 4 and 5. For the highest wave, $B_{\max} = 2.014007$, $a/\lambda = 0.713296$, $a/h = 5.703143$, $[X_p]/\lambda = 7.943256$ and $[X_q]/\lambda = 6.955806$. This wave in frame $P$ has trajectories as shown in figure 4. We present complete trajectories for $B/B_{\max} = 1$ and 0.75 in figure 4($a$) and for $B/B_{\max} = 0.5$, 0.35, 0.2, 0.1 and 0, together with part trajectories for $B/B_{\max} = 1$ and 0.75, in figure 4($b$). In figures 5($a$) and ($b$) we present the same particles as seen in frame $Q$. Immediately we see that as seen from frame $P$, particles travel further than the same particles viewed from frame $Q$. This emerges as a general characteristic of the relationship between the two frames. In both frames, particles in the free surface travel large relative distances and that as $B \to 0$, the profiles become more elliptic.

We now consider a thinner symmetric sheet ($k = 0.99$). For the highest wave, $B_{\max} = 0.794411$, $a/\lambda = 0.505016$, $a/h = 61997.51$, $[X_p]/\lambda = 12.571165$ and $[X_q]/\lambda = 2.048037$. The particle trajectories in frame $P$ are given in figure 6, for $B/B_{\max} = 1$, 0.5, 0.2 and 0. The considerable horizontal extent of the free-surface

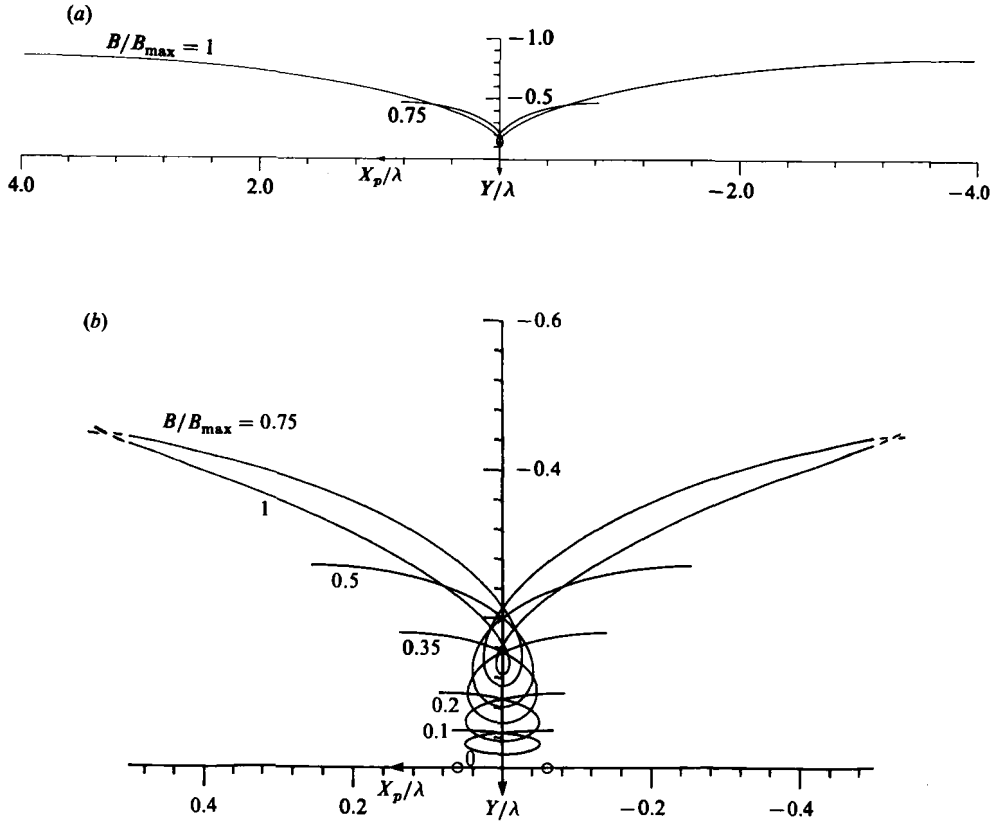


FIGURE 4. (a) Particle trajectories for symmetric ($k = 0.25$) capillary waves along streamlines $B/B_{max} = 1$ and 0.75 as seen in frame $P$. (b) Full trajectories for $B/B_{max} = 0.5$, 0.35, 0.2, 0.1 and 0 together with part trajectories from figure 3(a) as seen in frame $P$.

trajectory ($B/B_{max}$) makes illustration of the lower streamline trajectories very difficult. All the trajectories have a closed-loop section which is minute on this scale. With respect to frame $Q$, the picture is somewhat different as is shown in figure 7. The free surface trajectory is almost an open ellipse with the lower streamlines nearly closed. For $B = 0$, the particle trajectory is completely closed unlike the very open trajectory for $B = 0$ as seen in frame $P$, figure 6.

The case $k = 1$ for symmetric waves can also be considered. For frame $P$, it is straightforward to show that $c_p t/\lambda$ is infinite for all $B$. In fact for small $k'$ we show that

$$\frac{c_p t}{\lambda} \sim \ln \frac{4}{k'}, \tag{6.1}$$

For frame $Q$ the analysis is lengthier. We find, for $k = 1$,

$$\frac{c_q t}{\lambda} = \frac{3}{16 \sin^3 B \cos^3 B} \left\{ (2 \sin^2 B - 1) \tan^{-1} \left[ \frac{\tan B (E(\phi) + \tanh \phi)}{1 - E(\phi) \tanh \phi \tan^2 B} \right] \right.$$
$$\left. + \sin B \cos B \left[ E(\phi) + \frac{(1 + \sin^2 B \operatorname{sech}^2 \phi)}{(1 - \sin^2 B \operatorname{sech}^2 \phi)} \tanh \phi \right] \right\}. \tag{6.2}$$

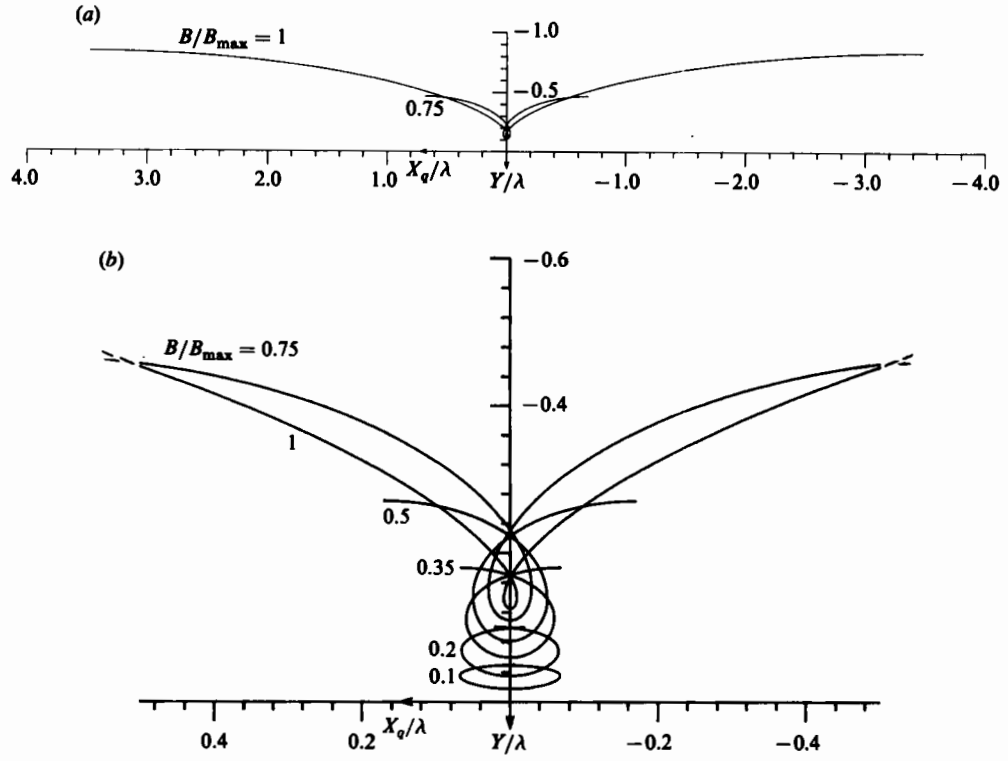


FIGURE 5. (*a*) As figure 4(*a*), as seen in frame $Q$. (*b*) As figure 4(*b*), as seen in frame $Q$.

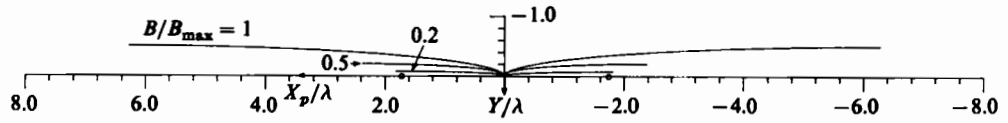


FIGURE 6. Particle trajectories for symmetric ($k = 0.99$) capillary waves along streamlines $B/B_{max} = 1$, 0.5, 0.2 and 0 as seen in frame $P$.

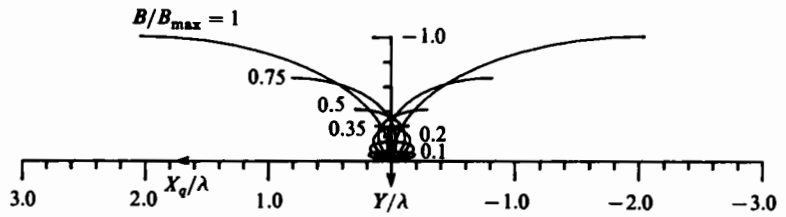


FIGURE 7. As figure 6, for $B/B_{max} = 1$, 0.75, 0.5, 0.35, 0.2, 0.1 and 0 as seen in frame $Q$.

The highest wave has $B = B_{max} = \frac{1}{4}\pi$ and hence we find in this case the simple result that

$$\frac{c_q T}{\lambda} = 3, \tag{6.3}$$

and hence that $[X_q]/\lambda = 2$ and $U_q/c_q = \frac{2}{3}$.

| $k$ | $\frac{a}{\lambda}$ | $\frac{a}{h}$ | $\frac{[X_p]}{\lambda}$ | $\frac{U_p}{c_p}$ | $\frac{[X_q]}{\lambda}$ | $\frac{U_q}{c_q}$ |
|---|---|---|---|---|---|---|
| (*a*) | | | | | | |
| 0 | 0.729765 | 0 | 7.995564 | 0.888834 | 7.995564 | 0.888834 |
| 0.25 | 0.713296 | 5.703143 | 7.943256 | 0.888184 | 6.955806 | 0.874306 |
| 0.5 | 0.666334 | 17.631155 | 7.855508 | 0.887076 | 4.939884 | 0.831647 |
| 0.75 | 0.594753 | 86.361970 | 8.032096 | 0.889284 | 3.222850 | 0.763193 |
| 0.9 | 0.541921 | 592.279268 | 8.881073 | 0.898796 | 2.449807 | 0.710129 |
| 0.99 | 0.505016 | 61997.506820 | 12.571165 | 0.926314 | 2.048037 | 0.671920 |
| 1 | 0.5 | $\infty$ | $\infty$ | 1 | 2 | 0.666667 |
| (*b*) | | | | | | |
| 0 | 0.729765 | 0 | 7.995564 | 0.888834 | 7.995564 | 0.888834 |
| 0.1 | 0.732467 | 2.503347 | 7.826048 | 0.886699 | 7.825599 | 0.886693 |
| 0.25 | 0.747825 | 4.016468 | 6.974659 | 0.874603 | 6.956960 | 0.874324 |
| 0.5 | 0.825805 | 6.135445 | 4.483467 | 0.817634 | 4.188386 | 0.807262 |
| 0.75 | 1.215003 | 9.325623 | 2.857299 | 0.740751 | 0.845197 | 0.458052 |
| 0.854 | 2.612856 | 355.668607 | 11.054501 | 0.917043 | 0.000230 | 0.000230 |
| 0.858517 | 2.820646 | $\infty$ | 13.168644 | 0.929422 | 0 | 0 |

TABLE 1. Parameters for complete orbits of surface particles (*a*) in highest symmetric (case I*b*) capillary waves on fluid sheets; (*b*) in antisymmetric (case II*b*) capillary waves.

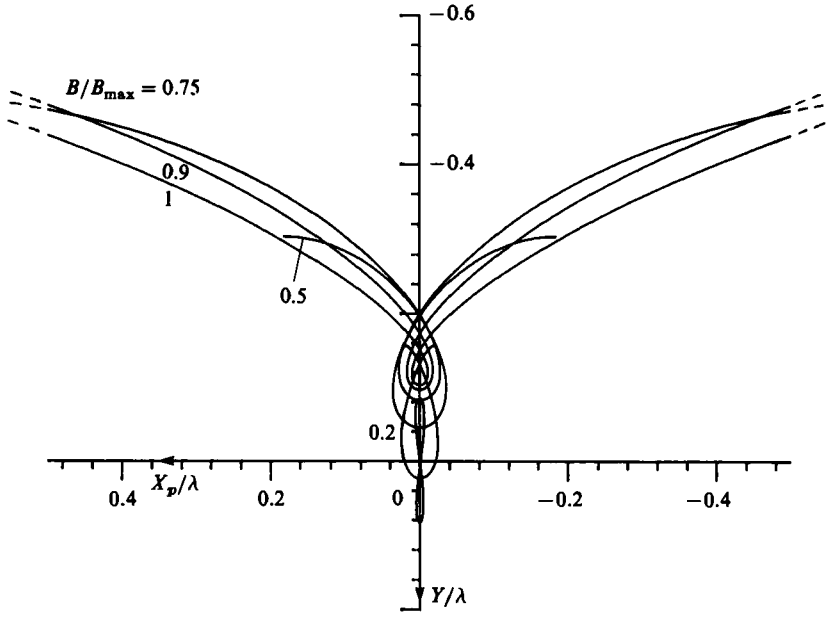


FIGURE 8. Particle trajectories for antisymmetric ($k = 0.25$) capillary waves along streamlines $B/B_{max} = 0.75$, 0.5, 0.2 and 0 together with part trajectories for $B/B_{max} = 1$ and 0.9 as seen in frame $P$.

As pointed out by Kinnersley, care must be taken in this case as only half the wave is covered by $\phi$ when $k = 1$. This is because $\operatorname{sn}\phi$ evaluated between the limits 0 and $4K$ gives the value zero whereas for $k = 1$ we must evaluate $\tanh\phi$ between 0 and infinity, giving the value one. This difficulty is surmounted by using at least two regions of $\phi$ and matching asymptotically.

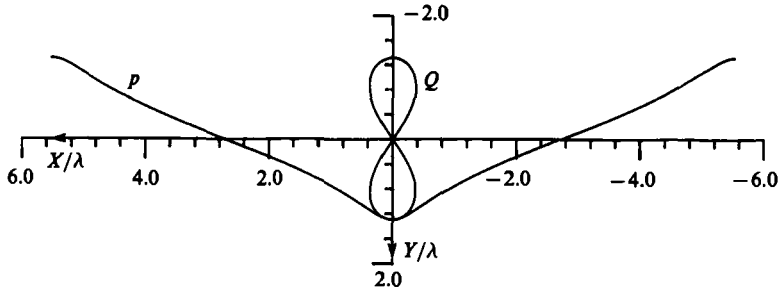


FIGURE 9. Particle trajectory for the antisymmetric ($k = 0.854$) capillary wave along free surface streamline as seen in both frames $P$ and $Q$.

The parameters for complete orbits of surface particles in the highest symmetric capillary waves on fluid sheets are given in table 1(*a*), together with information relevant to the wave profile itself. The results for $k = 0$ are taken from Hogan (1984) and correspond to nonlinear waves on a fluid of infinite depth.

We now consider antisymmetric waves (case II*b*). For $k = 0.25$ we give some of the particle trajectories, as viewed from frame $P$, in figure 8. This contains complete trajectories for $B/B_{\max} = 0.75$, 0.5, 0.2 and 0 together with part trajectories for $B/B_{\max} = 1$ and 0.9. This is quite similar to figure 4(*b*) except that the lower streamline trajectories are almost elliptic with a vertical major axis (in the symmetric case, the major axis was horizontal). The case $B = 0$ is an almost closed figure of eight. The full trajectories for $B/B_{\max} = 1$ and 0.9 have not been given as they are relatively long and are very similar to those of the symmetric wave for $k = 0.25$ in frame $P$. For the highest wave $B_{\max} = 1.986029$, $a/\lambda = 0.747825$, $a/h = 4.016468$, $[X_p]/\lambda = 6.974659$ and $[X_q]/\lambda = 6.956960$.

We have not given the trajectories of the antisymmetric wave with $k = 0.25$ as seen from frame $Q$ as they are almost identical to those as seen from frame $P$, since $c_p \approx c_q$ in this case.

As $k$ increases to the physical limit of 0.858517, the differences in the trajectories between the two frames become more marked. For $k = 0.854$, the highest wave has $B_{\max} = 0.009685$, $a/\lambda = 2.612856$, $a/h = 355.6686$, $[X_p]/\lambda = 11.054501$ and $[X_q]/\lambda = 0.000230$. The trajectories for $B = B_{\max}$ as seen from both frames $P$ and $Q$ are given in figure 9. Other trajectories are very similar and lead to confusion if superimposed. This is because $B_{\max}$ is so small and the wave so thin. There is a tiny closed section in the trough of the trajectory as seen from frame $P$.

For both wave symmetries we have omitted one half of the complete trajectory. Thus for symmetric waves a simple inversion of the trajectories as given in figures 4–7 is required. For antisymmetric waves, the trajectories of figures 8 and 9 should be translated by $\pm[X]/2\lambda$ and then inverted.

We now consider the behaviour of the time-averaged drift velocity ratio $U_p/c_p$ as a function of $(\bar{y}_0 - \bar{y}_c)/\lambda$. Figure 10(*a*) contains the results for symmetric waves. The case $k = 0$ is included for reference. The case $k = 1$ consists of a vertical straight line along $U_p/c_p = 1$ between $(\bar{y}_0 - \bar{y}_c)/\lambda = 0$ and $-\frac{1}{8}\pi$. Clearly as the sheet becomes thinner the drift velocity ratio increases along the centre streamline. The behaviour at the free surface is more complicated, with an initial decrease from the value 0.888834 at $k = 0$ followed by an increase up to $U_p/c_p = 1$ at $k = 1$. It is remarkable how little change there is in $U_p/c_p$ from $k = 0$ to $k = 0.9$, at least for $(\bar{y}_0 - \bar{y}_c)/\lambda$ between 0 and $-0.4$.

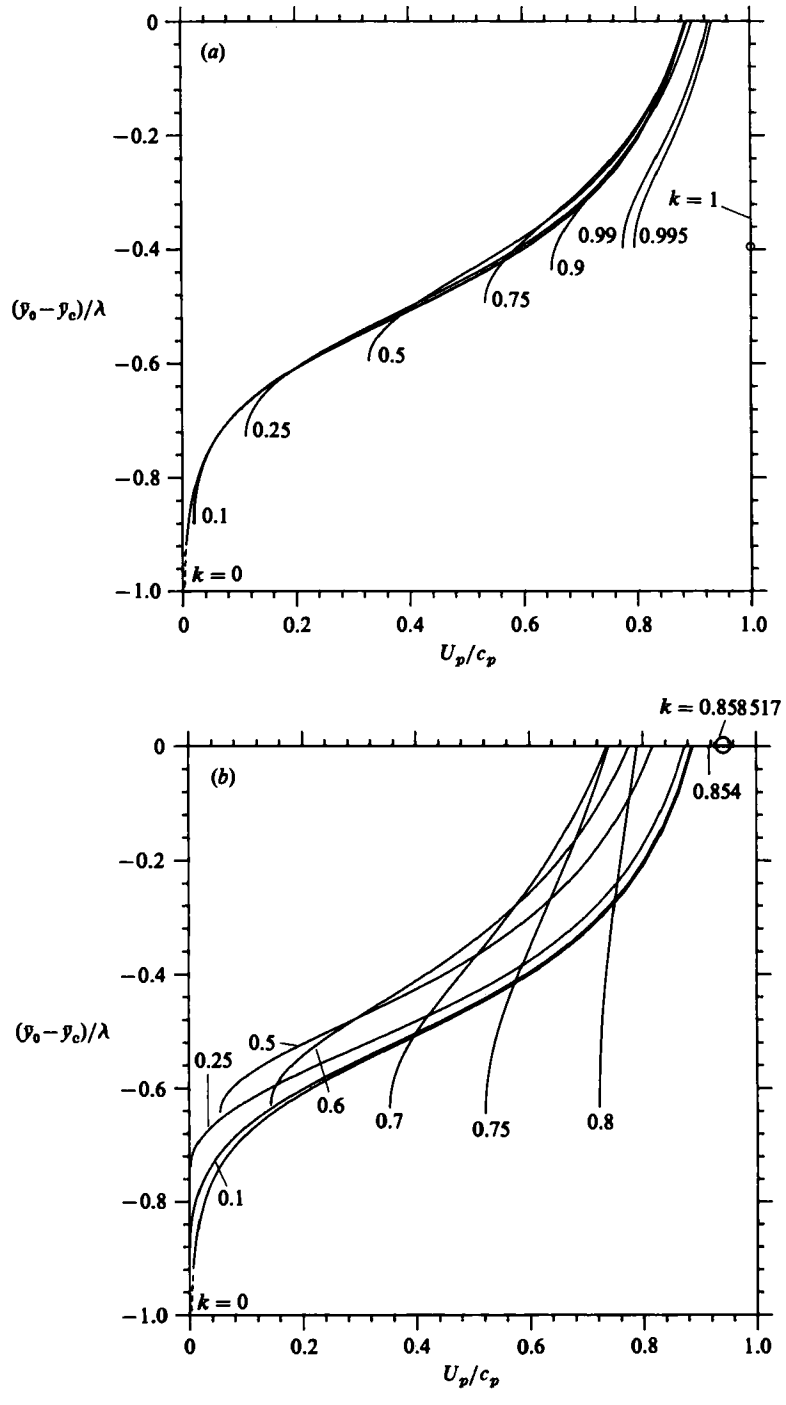


FIGURE 10. (*a*) Drift velocity ratio $U_p/c_p$ as a function of the mean displacement of fluid particles $(\bar{y}_0-\bar{y}_c)/\lambda$ for symmetric capillary waves ($k = 0$, 0.1, 0.25, 0.5, 0.75, 0.9, 0.99, 0.995 and 1). (*b*) As figure 10(*a*), for antisymmetric capillary waves ($k = 0$, 0.1, 0.25, 0.5, 0.6, 0.7, 0.75, 0.8, 0.854). The point marked ○ corresponds to the limiting case $k = 0.858517$.

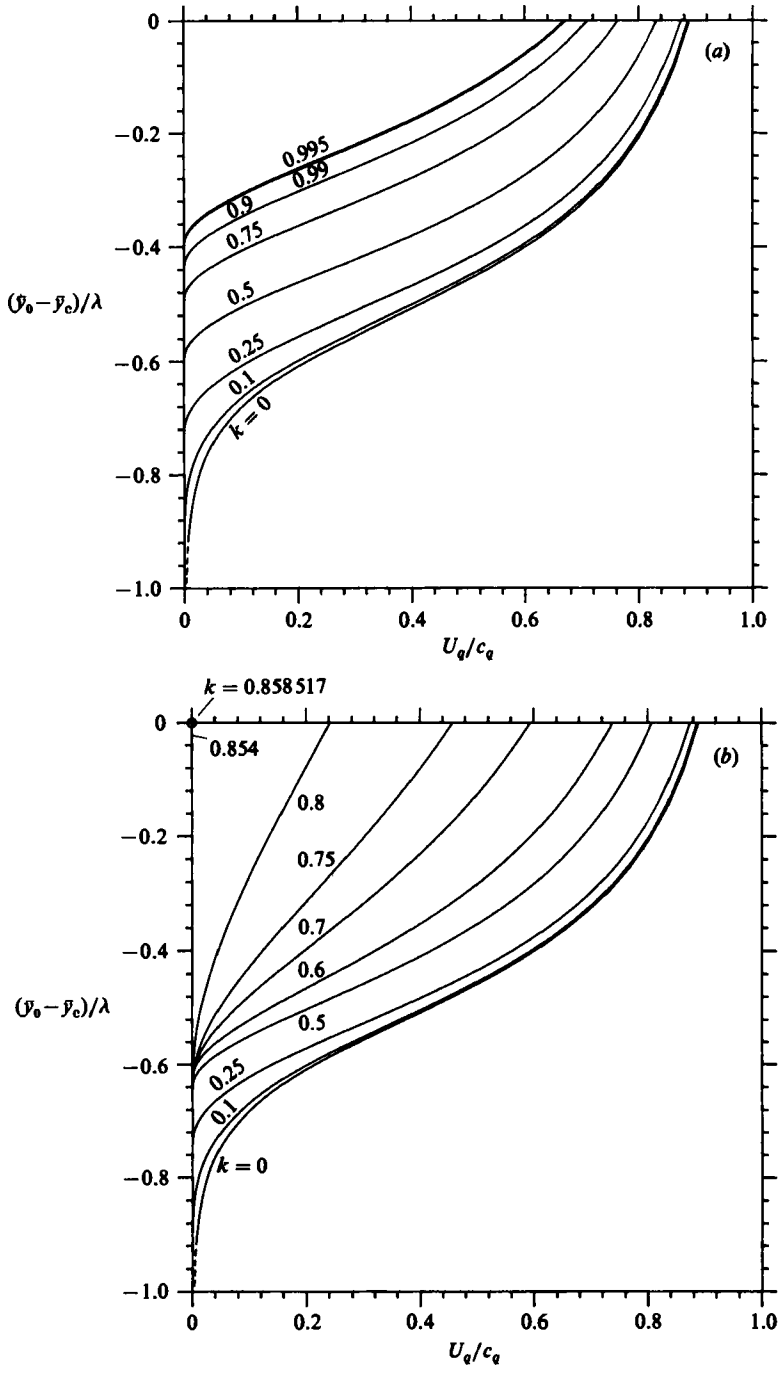


FIGURE 11. (*a*) As figure 10(*a*) for $U_q/c_q$. (*b*) As figure 10(*b*) for $U_q/c_q$.

Figure 10(*b*) contains results for antisymmetric waves, again with the case $k = 0$ included for reference. Here the behaviour is more complicated than in figure 10(*a*). Although a little difficult to determine on this scale, there is a non-zero drift of the centreline for $k = 0.1$ and 0.25. For $k = 0.5$, the surface drift has decreased but the centre drift has increased considerably. At $k = 0.75$, the coordinates of the free

surface have undergone a change that leads to an increase in the surface value of $(\bar{y}_0-\bar{y}_c)/\lambda$. Specifically the $y$-coordinates of particles near the crest have begun to increase after a gradual decrease from $k=0$ whereas the $y$-coordinates of particles near the trough have continued to increase. In fact the wave profile has an almost constant thickness along its length and so $U_p/c_p$ is nearly constant. Then physical constraints begin to act and at $k=0.854$, the sheet is very thin, of almost uniform thickness and $U_p/c_p$ is constant to within 0.005%. At the limit, the value of $U_p/c_p$ is 0.929422.

We now consider the behaviour of $U_q/c_q$. As with $U_p/c_p$, the case $k=0$ is included for reference. For symmetric waves, we present the results in figure 11 (*a*). The case $k=1$ extends from the point $[U_q/c_q, (\bar{y}_0-\bar{y}_c)/\lambda] = (\frac{2}{3}, 0)$ to the point $(0, -\frac{1}{8}\pi)$. In general the free-surface values of $U_q/c_q$ decrease monotonically. It is difficult to distinguish the cases $k=0.99$ and $k=0.995$, unlike in figure 10 (*a*).

The results for $U_q/c_q$ for antisymmetric waves are given in figure 11 (*b*). The case $k=0.854$ does not show up on this scale. The limiting case $k=0.858517$ is at the origin.

We note that between figures 10 and 11, the values of $(\bar{y}_0-\bar{y}_c)/\lambda$ are unchanged, being dependent on $k$ rather than $c_p$ or $c_q$.

The classical result (Stokes 1847 equation (24)) was derived for the symmetric case only. The order of the approximation was such as explained by Stokes, that either definition $c_p$ or $c_q$ of the phase velocity could be used. Thus he found

$$\frac{U_p}{c_p} = \frac{U_p}{c_q} = \frac{\pi^2 \cosh\left[(4\pi/\lambda)(y-h)\right]}{2\sinh^2\left[2\pi h/\lambda\right]}\left(\frac{a}{\lambda}\right)^2. \tag{6.4}$$

We find that this result overpredicts considerably not only at the free surface as found in Hogan (1984) but also for the centreline drift.

## 7. Discussion

We have generalized the work of Hogan (1984) to examine the effects of finite depth on the trajectories of pure capillary waves. We used the exact solutions for the wave profiles derived by Kinnersley (1976). We have extended and amended his work. In particular we have presented highest waves in graphical form, using an explicit criterion derived by us. We have also shown that the phase velocity does not equal Kinnersley's constant $c$. In this way the 'essentially nonlinear' waves of Kinnersley are shown to have been misinterpreted. In fact instead of a strong dependence on wave steepness, the phase speed of these limiting waves turns out to be zero according to either of Stokes' definitions.

In frame $P$, for both types of wave on a fluid sheet, a decrease in sheet thickness leads to a non-monotonic behaviour in global trajectory properties. The relative distance travelled $[X_p]/\lambda$ at first decreases from the infinite depth result and then increases again as the sheet thickness decreases. For symmetric waves, the increase is without limit whereas for antisymmetric waves there is a physical cutoff. A similar pattern holds for $U_p/c_p$ except that for symmetric waves the limit is equal to one and for antisymmetric waves, slightly less than one.

In frame $Q$, the behaviour is monotonic. Thus, $[X_q]/\lambda$ at the free surface decreases from 7.995564 at $k=0$ to 2 at $k=1$ for symmetric waves and to zero for antisymmetric waves. Similarly $U_q/c_q$ decreases from 0.888834 at $k=0$ to $\frac{2}{3}$ at $k=1$ for symmetric waves and to zero for antisymmetric waves.

Physically it is difficult to imagine that the limiting cases can be sustained. In

particular Matsuuchi (1974) has shown that the wavetrains are modulationally unstable. His analysis is not valid for arbitrary steepness or arbitrary perturbation wavelength. Viscosity and surface tension gradients will affect the behaviour as discussed in Hogan (1984).

The propagation of waves over a solid boundary can be modelled by using the top half of the symmetric solution with the boundary coincident with the dividing streamline. Here however boundary-layer development may well affect our conclusions, growing quickly to swamp the inviscid core region when the sheet thickness is small. Nevertheless, these results may be of interest for wave propagation in thin films of fluid adhering to pipe walls. We conclude that particles can move enormous relative distances at high average speed along a pipe wall throughout the film thickness, rather than just at the surface.

The author gratefully acknowledges support in the form of a Junior Research Fellowship from King's College, Cambridge where this work was begun. It was concluded while the author was CEGB Research Fellow at St Catherine's College, Oxford. Dr D. H. Peregrine's comments on an earlier version of this paper led to the inclusion of §4.

## REFERENCES

Byrd, P. F. & Friedman, M. D. 1971 *Handbook of Elliptic Integrals for Engineers and Scientists*, 2nd edn. revised. Springer.

Crapper, G. D. 1957 An exact solution for progressive capillary waves of arbitrary amplitude. *J. Fluid Mech.* **2**, 532–540.

Hogan, S. J. 1984 Particle trajectories in nonlinear capillary waves. *J. Fluid Mech.* **143**, 243–252.

Hogan, S. J. 1985*a* Particle trajectories in nonlinear gravity-capillary waves. *J. Fluid Mech.* **151**, 105–119.

Hogan, S. J. 1985*b* Particle trajectories in nonlinear capillary waves. In *The Ocean Surface: Wave Breaking, Turbulent Mixing and Radio Probing* (ed. Y. Toba & H. Mitsuyasu), pp. 25–30. Dordrecht: D. Reidel.

Kinnersley, W. 1976 Exact large amplitude capillary waves on sheets of fluid. *J. Fluid Mech.* **77**, 229–241.

Longuet-Higgins, M. S. 1979 The trajectories of particles in steep, symmetric gravity waves. *J. Fluid Mech.* **94**, 497–517.

Matsuuchi, K. 1974 Modulational instability of nonlinear capillary waves on thin liquid sheet. *J. Phys. Soc. Japan* **37**, 1680–1687.

Stokes, G. G. 1847 On the theory of oscillatory waves. *Trans. Camb. Phil. Soc.* **8**, 441–455.

Taylor, G. I. 1959 The dynamics of thin sheets of fluid. II. Waves on fluid sheets. *Proc. R. Soc. Lond.* A**253**, 296–312.